Anomalous supercooled liquid structure of Ga on β-relaxation dynamics

H. C. Chen and S. K. Lai
Department of Physics, National Central University, Chung-li 32054, Taiwan, Republic of China
(Received 30 December 1996; revised manuscript received 16 April 1997)

We study the β-relaxation dynamics for liquid metal gallium using computer-simulated liquid structures in conjunction with idealized mode-coupling theory. At the dynamical transition point, our calculated mode-coupling parameter λ is numerically more consistent with the increasing trend of the magnitude of the experimentally fitted λ (~ 0.8) observed in several glass-forming materials. The implication is that the empirically fitted λ inherently must contain contributions arising from other subtle mechanisms to the β-relaxation dynamics in addition to the usual cage-diffused mechanism. Of particular interest in our calculations is the behavior of the tagged particle distribution function, which shows a distinct double-peaked structure and, within the β-relaxation time regime, exhibits a much slower retarded motion compared with other simple monatomic systems. This curious behavior is interpreted here as due to the influences of temporally fluctuating atomic bonded-pair clusters that have been observed recently in molecular dynamics simulations.
[S1063-651X(97)03110-3]

PACS number(s): 64.70.Pf, 61.20.Lc, 61.25.Mv

I. INTRODUCTION

The dynamics of supercooled liquids is an active area of current experimental and theoretical interest. Experimentally both light- and neutron-scattering techniques [1] have made tremendous progress in enriching our knowledge of the variety of relaxation phenomena prevailing in many glass-forming materials. Theoretically, mode-coupling theory (MCT) [2,3], which is a formal generalization of the kinetic theory of an equilibrium liquid and of Vlasov plasma theory, has in recent years received considerable attention. This theory was originally proposed for studying the basic dynamics of monatomic supercooled liquids at a microscopic level, although in subsequent development it has been extended to two component mixtures [4–6]. In this connection, it is perhaps worthwhile to point out that the theory has commonly been used also by experimentalists [1] in interpreting dynamic data for far more sophisticated multicomponent systems. Many of these experimental applications are, however, theoretically in doubt since the mode-coupling exponent constants are treated there as mere fitting parameters which thus leave obscure the physical meaning of the microscopic details buried in the parameters. It is one of the purposes of this paper to calculate directly an instructive mode-coupling parameter λ (to be defined below) and to study, within MCT, the temporal evolution of the density-density fluctuations that are uniquely determined by λ. But differing from several recent works [7–11], we focus on liquid metal gallium for the following specific reasons.

The structure of liquid metal gallium is in many respects unique. This system has a low melting temperature ($T_m \approx 303$ K), but among other pure simple liquid metals, it can be supercooled very considerably and can form an amorphous solid relatively more easily [12]. Structurally, as Fig. 1 shows, this element exhibits anomalous undercooled characteristics with the main maximum of the static liquid structure factor $S(q)$ displaying a pronounced shoulder near T_m which develops into a double-peaked splitting at lower supercooled temperatures [13]. This curious phenomenon differs somewhat from commonly observed quenched systems where it is the second principal peak of $S(q)$ that exhibits the shoulder-like two-peaked feature. From the structural point of view, this would imply a more ordered atomic distribution for the supercooled states of Ga. In this respect it is of great theoretical interest to apply MCT to this metal since the theory has $S(q)$ as the sole input and the principal peak of $S(q)$ plays a decisive role in the underlying physics of MCT. The main aim of this work is to study within idealized MCT the dynamics of the supercooled liquid Ga in the vicinity of the dynamical transition point T_c. Through comparing the calculated λ and relevant correlation functions at or near T_c with those from other model systems such as the hard spheres [9,8], Lennard-Jones atoms [10] and Lennard-Jones binary mixtures [4,5], binary soft spheres [6], liquid metals Na and K [7,8], liquid dimers [11], and fused salt $[Ca(NO_3)_2]_{0.4}[KNO_3]_{0.6}$ [14], we explore the subtle effects of microscopic interactions and of geometric factors on the supercooled liquid dynamics within MCT.

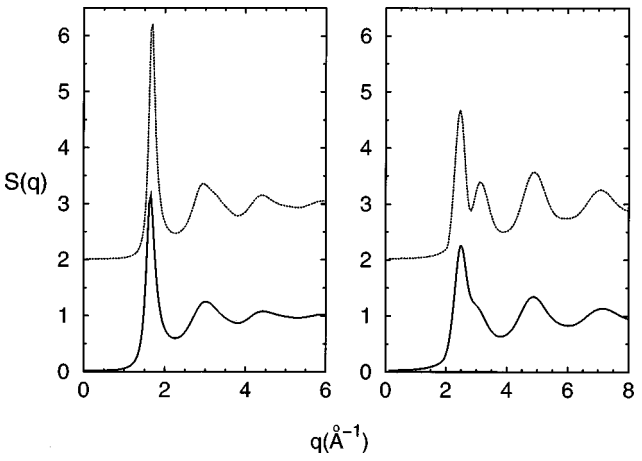

FIG. 1. Static structure factors $S(q)$ for liquid metals potassium (left) and gallium (right) near freezing (full curve) and at the dynamical transition temperature (dotted curve).

 © 1997 The American Physical Society

II. MODE-COUPLING THEORY: β RELAXATION

Central to MCT is the real-time normalized density-density fluctuation function $R(q,t)=\langle \delta\rho(\mathbf{q},t)\delta\rho(-\mathbf{q},0)\rangle/S(q)$ where $\delta\rho$ is the density fluctuation from the equilibrium density ρ_0. The Laplace transform of $R(q,t)$ which is defined by $\hat{R}(q,z)=i\int_0^\infty dt\ \exp(izt)R(q,t)$ satisfies [3]

$$\hat{R}(q,z)=-\frac{z+\hat{M}(q,z)}{z^2-q^2/\beta mS(q)+z\hat{M}(q,z)}. \tag{1}$$

Here $\beta=1/(k_BT)$ is the inverse temperature, m is the mass of the particle, and $\hat{M}(q,z)$ is the memory function. In idealized MCT one focuses on long-time behavior, which amounts to ignoring the short-time part of $M(q,t)$ and approximating $M(q,t)\approx\Lambda(q,t)$ [2,7] by

$$\begin{aligned}\Lambda(q,t)=&\frac{\rho_0}{8mq\beta\pi^2}\int_0^\infty dq'q'\int_{|q'-q|}^{|q'+q|}dq''q''\\&\times\left(\frac{q'^2-q''^2}{2q}[c(q')-c(q'')]\right.\\&\left.+\frac{q}{2}[c(q')+c(q'')]\right)^2S(q')S(q'')\\&\times R(q',t)R(q'',t),\end{aligned} \tag{2}$$

in which $\rho_0c(q)=1-1/S(q)$ is the direct correlation function. Given $S(q)$ MCT predicts an ergodic-nonergodic transition at T_c that is determined by solving the nonlinear equation [2]

$$\frac{f(q)}{1-f(q)}=\frac{\beta mS(q)}{q^2}\Lambda(q,t\to\infty)\equiv\mathcal{F}_q(f(k)) \tag{3}$$

for the Debye-Waller factor, $f(q)=0$ for the ergodic state, and $f_c(q)=R(q,t\to\infty)\neq0$ for the nonergodic state.

Further, it is shown in MCT that, near T_c, $R(q,t)$ deviates from $f_c(q)$ and within the mesoscopic time scale ($t_\beta\simeq10^{-11}$ s–10^{-9} s) of the β-relaxation process can be factorized into a product of the temporal and spatial parts as

$$R(q,t)=f_c(q)+h_c(q)\mu\sqrt{1-\lambda}\sqrt{|\varepsilon|}G_\pm(t/t_\beta), \tag{4}$$

where $\varepsilon=(T_c-T)/T_c$; $h_c(q)=[1-f_c(q)]^2l_q^c$ is the critical amplitude [3,9,8], l_q^c (or $\hat{l}_q^c$) being the right-hand (or left-hand) eigenvector of the stability matrix $C_{qk}=[1-f(k)]^2\partial\mathcal{F}_q/\partial f(k)$ and $\mu^2=[\Sigma_q\hat{l}_q^cT_c(\partial\mathcal{F}_q/\partial T)_{f(k)}]/(1-\lambda)$. Here the material-dependent λ is defined by

$$\begin{aligned}\lambda=&\frac{1}{2}\sum_{q,k',k''}\hat{l}_q^c[1-f(k')]^2[\partial^2\mathcal{F}_q/\partial f(k')\partial f(k'')]_T\\&\times[1-f(k'')]^2l_{k'}^c,l_{k''}^c\end{aligned} \tag{5}$$

and when substituted into

$$\mp1+\zeta^2\hat{G}_\pm^2(\zeta)+\lambda\zeta i\int_0^\infty d\tau e^{i\zeta\tau}G_\pm^2(\tau)=0, \tag{6}$$

$\zeta=zt_\beta$ and $\tau=t/t_\beta$ being rescaled variables, uniquely determines the scaled master function $G_\pm(t/t_\beta)$ [3]. In Eq. (6) the subscripts plus and minus in $G_\pm(t/t_\beta)$ refer to glassy $\varepsilon>0$ and liquid $\varepsilon<0$ sides of T_c, respectively. Note that the rescaled time $t_\beta=t_0|\mu^2(1-\lambda)\varepsilon|^{-1/(2a)}$ where $t_0\simeq10^{-14}$ s is the microscopic time and the exponent parameter a can be determined from

$$\lambda=\Gamma^2(1-a)/\Gamma(1-2a) \tag{7}$$

in terms of the gamma function $\Gamma(x)$.

The same logic extends to the tagged particle correlator whose $R^s(q,t)$ can be shown to read

$$R^s(q,t)=f_c^s(q)+h_c^s(q)\mu\sqrt{1-\lambda}\sqrt{|\varepsilon|}G_\pm(t/t_\beta), \tag{8}$$

where $R^s(q,t)=\langle\delta\rho^s(\mathbf{q},t)\delta\rho^s(\mathbf{0},0)\rangle$. Here $h_c^s(q)$ is the tagged particle critical amplitude and f_c^s is the Lamb-Mössbauer factor, the solution of the following equation [8]:

$$\frac{f^s(q)}{1-f^s(q)}=\frac{m\beta}{q^2}\Lambda^s(q,t\to\infty)\equiv\mathcal{F}_q^s(f^s(k),f(k')) \tag{9}$$

where

$$\begin{aligned}\Lambda^s(q,t)=&\frac{\rho_0}{16\pi^2m\beta q^3}\int_0^\infty dq'q'\\&\times\int_{|q-q'|}^{|q+q'|}dq''q''[q'^2+q^2-q''^2]^2c^2(q')\\&\times S(q')R(q',t)R^s(q'',t).\end{aligned} \tag{10}$$

Note that in solving Eqs. (9) and (10) self-consistently for $f_c^s(q)$, one requires $f(q)$ as an input. It is obvious that, once the dynamical transition point is located, λ (and other mode-coupling parameters) can be calculated readily and the asymptotic dynamic solutions near T_c [3,7] follow straightforwardly.

III. NUMERICAL RESULTS AND DISCUSSION

Equations (2) and (3) have been solved iteratively and self-consistently by utilizing the $S(q)$ obtained by Fourier transforming the computer-simulated pair correlation function $g(r)$ at various supercooled temperatures [13]. We find that the dynamical transition point for Ga occurs at $T_c=114.32$ K. This value of T_c is of order if one analyzes the time dependence of the mean-square displacement (see Fig. 3 in Ref. [13]), which indicates a cessation in diffusive motion of atoms at $T\simeq100$ K. Note that for Ga metal we have not assessed the consistency of T_c from the Wendt-Abraham-type transition temperature [7,8] since there is no transition ''kink'' for the Wendt-Abraham parameter R [defined as the ratio of the first minimum to the first maximum of $g(r)$] versus the T plot [15]. We attribute this departure of R from the usual behavior to the more subtle structure which this metal possesses in the supercooled states. In fact, as demonstrated by Tsay [13], the structure of Ga predominantly consists of 1201-type atomic bonded-pair clusters [16] which are quite different from the 1551-type icosahedral clusters (see the schematic diagrams given in Fig. 2) prevail-

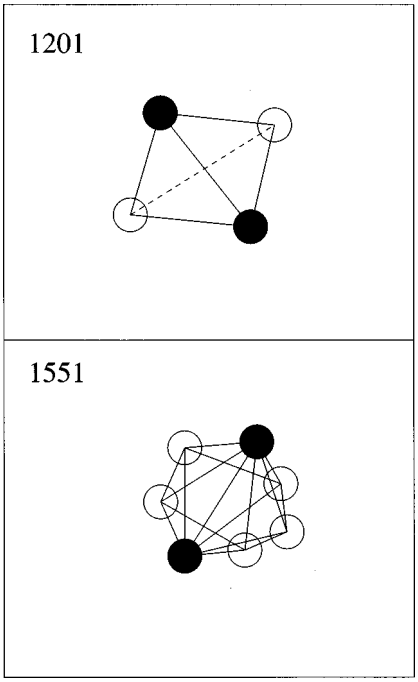

FIG. 2. Schematic diagrams for the 1201- and 1551-type bonded-pair atomic clusters. Reference [16] should be consulted for the nomenclature.

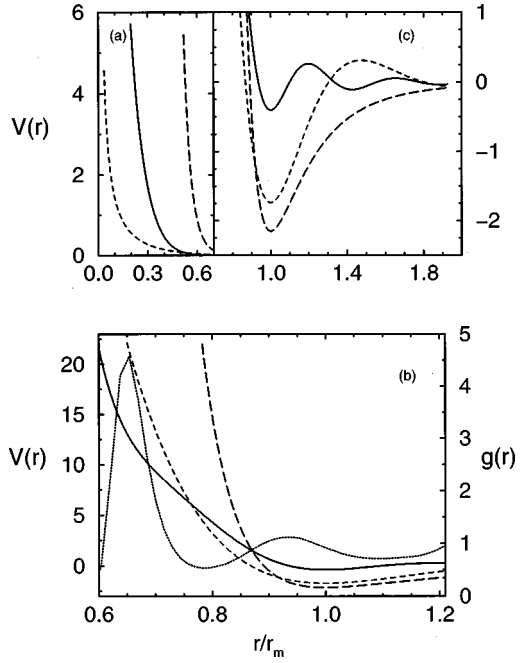

FIG. 3. Interatomic pair potential $V(r)$ of Lennard-Jones atoms (long-dashed curve) and liquid metals potassium (short-dashed curve) and gallium (full curve) for (a) the repulsive part, scaled to the first minimum $V(r_m)$ at the first minimum position r_m in units of $10^3 k_B T$ for $r<0.6r_m$, (b) same as (a) without scaling to $V(r_m)$ and in units of $k_B T$ for $0.6r_m \lesssim r \lesssim 0.9r_m$, and (c) same as (b) for the attractive tail $r>0.9r_m$. To manifest the ledge-shape region for Ga, we display in (b) its relation with the structure of the pair correlation function $g(r)$ (dotted curve).

ing in most amorphous solids.

Applying Eq. (5) we obtain $\lambda=0.739$. This value lies between the hard-spheres $\lambda_{\mathrm{HS}}=0.772$ [8] and the Lennard-Jones $\lambda_{\mathrm{LJ}}=0.718$ [10], but is larger than those of the liquid metals Na and K, namely, $\lambda_{\mathrm{Na}}=0.712$ and $\lambda_{\mathrm{K}}=0.710$ [8]. To understand these differences in λ values let us compare in Fig. 3 the pair potential $V(r)$ for the Lennard-Jones atoms, and liquid metals K and Ga. It can be seen that the $V(r)$ of Ga exhibits a rather complex structure; it displays a strong repulsive part [Fig. 3(a)] for $r \lesssim 0.6r_m$, r_m being the first minimum position, then shifts to a ledgelike feature [Fig. 3(b)] for $0.6r_m \lesssim r \lesssim 0.9r_m$, and prolongs to a *distinctly* weak attractive part [Fig. 3(c)] tailing with the typical Friedel oscillation for $r>0.9r_m$. The repulsive force resembles the hard spheres whose λ tend to be large [9,8] while the relatively weak attractive tail mimics a system of Lennard-Jones atoms and liquid alkali metals whose λ tend to reduce markedly [8,10]. From these two basic features, one would judge from the details in interparticle interactions (behaviors of strongly repulsive and weakly attractive) a comparatively smaller λ for Ga than for the liquid metal K. We notice, however, that the λ of Ga does not follow the expected decreasing trend [11,10]. This implies that the ledge-shape range $0.6r_m \lesssim r \lesssim 0.9r_m$ of $V(r)$, which is absent in most monatomic systems, must be playing a subtle and delicate role in the liquid structures of Ga. Indeed, as shown in Fig. 3(b), the principal maximum of the pair correlation function $g(r_{1,\max})$ falls in this range, which is quite different from many commonly observed monatomic systems (either Lennard-Jones atoms or other simple liquid metals) where the first minima of $V(r_m)$ and $g(r_{1,\max})$ coincide. We defer discussing its significance on λ below.

To pursue our analysis further, we depict in Fig. 4 the tagged particle distribution function $P^s_{\pm}(r,t)=4\pi r^2 R^s(r,t)$ for Ga in both the liquid ($\varepsilon<0$) and the glassy ($\varepsilon>0$) regions. The striking feature is that near T_c there occurs a distinct subpeak at the falling edge of the main maximum of $P^s_{\pm}(r,t)$, whereas no such corresponding second peak exists for either the hard spheres [17,8] or liquid metals Na and K [8]. As a result, the $P^s_{\pm}(r,t)$ of Ga exhibit somewhat different features with the $P^s_{-}(r,t)$ showing a much slower retarded tendency and the $P^s_{+}(r,t)$ revealing a typical localized motion. The explanation for this curious phenomenon can be traced to the anomalous supercooled states of Ga which are seen [13] in the simulation to consist of temporally fluctuating atomic clusters [16] predominantly of 1201 type and less prevalently of 1311 and 1301 type. In each of these atomic bonded-pair clusters the root pair atoms (see Ref. [16] for the nomenclature), are each bonded to two (1201-type) or three (1311- or 1301-type) common neighbors which themselves may be bonded (1311-type) or unbonded (1201- and 1301-type) atoms. In this geometric distribution, apart from giving rise to the cage-effect diffusive mechanism, these temporally bonded nearest-neighbor atoms have an additional influence on the tagged particle which will respond to any possible change arising from its intimate association with these bonded atoms. Accordingly, it is *likely* that the cage-diffusive behavior for $P^s_{\pm}(r,t)$ will unavoidably be affected by its bonded-pair atoms whose presence makes the appearance of the second peak in $P^s_{\pm}(r,t)$ realistic. Thus, as time evolves and within the β-relaxation regime, one finds (a) generally as in other monatomic systems, that $P^s_{\pm}(r,t)$ decreases (increases) in magnitude for $r<(>)0.16\sigma$ (here

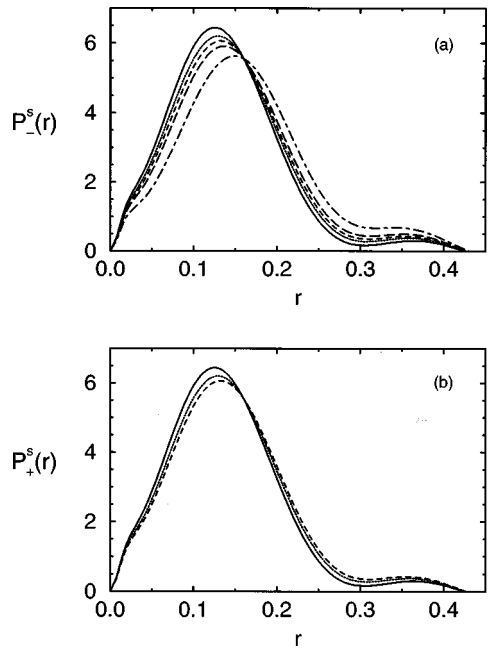

FIG. 4. Tagged particle distribution function $P^s_{\pm}(r)$ vs r (in units of σ) for liquid metal gallium near the dynamical transition point T_c at (a) $\tau_i = t_i/t_\beta = 5\times10^{-3+i}$ for $i=0$ (full curve), 1 (dotted curve), 2 (short-dashed curve), 3 (long-dashed curve), and 4 (chain curve) in the $\varepsilon<0$ ergodic region and (b) $\tau_{i+4}=t_i/t_\beta=10^{-3+i}$ for $i=1$ (full curve), 2 (dotted curve), and 3 (dashed curve) in the $\varepsilon>0$ nonergodic region.

the hard-sphere diameter σ is evaluated at $\eta=\pi\sigma^3\rho_0/6=0.5324$ [8]) indicating an attempt of the tagged particle to push its way through the surrounding cage of nearest-neighbor particles and (b) concurrently, that $P^s_{\pm}(r,t)$ is bond hindered by the latter manifesting in a gradual development of the second subpeak of $P^s_{\pm}(r,t)$.

To gain further insight into this complex behavior, let us focus on the positions of the first and second maxima of $P^s_{\pm}(r,t)$, namely, at $r^{(1)}_{\max}\simeq0.134\sigma$ and $r^{(2)}_{\max}\simeq0.354\sigma$, respectively. These positions yield a separation approximately 0.22σ which is roughly the region the temporally bonded atoms can ''straddle'' [18] and, due to their intimate ''bonding''association with the tagged particle, can induce a bond-hindered mechanism superimposed on the supposedly cage-diffused motion. Table I gives further details of the change in time of $r^{(2)}_{\max}$; these data illustrate that, as time elapses, $P^s_{\pm}(r^{(2)}_{\max},t)$ increases in height and moves inward. It is interesting to note here that this subtle two-peaked structure is reminiscent of the simulation results of the fused salt $[Ca(NO_3)_2]_{0.4}[KNO_3]_{0.6}$ whose $P^s_{\pm}(r,t)$ of oxygen in NO_3 ions (see Fig. 6 in Ref. [14]) reveal similar two-peaked structure and were demonstrated there to be due to rotation. Although the bonded-pair atomic clusters for Ga (either the predominant 1201 type or the less prevalent 1301 and 1311 types) are temporally fluctuating, the average picture described above may have some relevance to this same physical origin. We should emphasize, however, that double-peaked structure reported here is not due to the thermal-activated process since the idealized MCT does not *a priori* include this contribution in the theoretical formulation. At this point it is clear that $\lambda=0.739$, which does not follow the expected trend of a decreasing λ for increasing ''*complexity*'' in interparticle interactions [8,10,11], is now evidenced to be partly due to an additional bond-hindered mechanism arising from the possible impediment induced by bonded-pairs atoms. Such a conjecture is not unreasonable given that the observed trend of the magnitude of the experimentally fitted λ is generally large (~0.8) and that the laboratory glass-forming materials are structurally more susceptible to the above ''bonding'' picture.

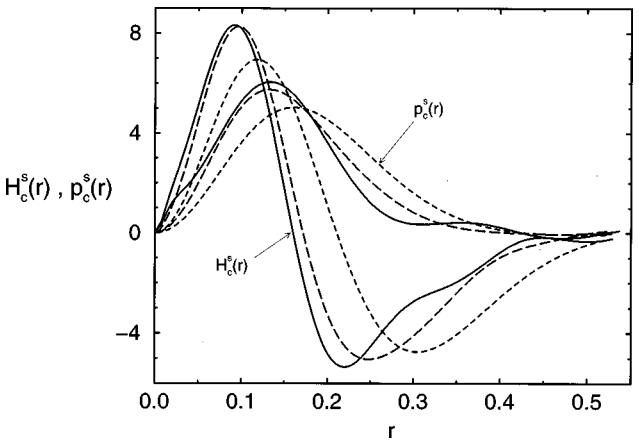

FIG. 5. Spatial functions $H^s_c(r)$ and $p^s_c(r)$ of the tagged particle distribution function vs r (in units of σ) for gallium (full curve), potassium (short-dashed curve), and the hard-sphere system (long-dashed curve).

Finally, we present in Fig. 5 the spatial distribution functions of the $p^s_c(r)=4\pi r^2 f^s_c(r)$ and $H^s_c(r)=4\pi r^2 h^s_c(r)$ given in Eq. (8) for the hard-sphere model and liquid metals K and Ga. An interesting feature is the close resemblance of the $p^s_c(r)$ and $H^s_c(r)$ for the Ga and hard-sphere particles, which both differ somewhat from the liquid metal K. These differences can be understood qualitatively from the pair potential given in Fig. 3(a). Notice, however, that there is a discernible broad peak for $p^s_c(r)$ in the range $0.3\sigma<r<0.42\sigma$. This conspicuous peak is partly the origin for the second peak of

TABLE I. Tagged particle distribution function $P^s_{\pm}(r^{(2)}_{\max},\tau_i)$ of liquid metal Ga evaluated at the second maximum position $r^{(2)}_{\max}$ at $\tau_i = t_i/t_\beta = 5\times10^{-3+i}$ for $i=0,\ldots,4$ in the $\varepsilon<0$ ergodic region and at $\tau_{i+4}=t_i/\tau_\beta=10^{-3+i}$ for $i=1,\ldots,3$ in the $\varepsilon>0$ nonergodic region. σ is defined in text.

	Ergodic					Nonergodic		
	τ_0	τ_1	τ_2	τ_3	τ_4	τ_5	τ_6	τ_7
$r^{(2)}_{\max}/\sigma$	0.364	0.359	0.355	0.351	0.340	0.364	0.359	0.355
$P^s_{\pm}(r^{(2)}_{\max},\tau_i)$	0.298	0.374	0.425	0.488	0.676	0.298	0.374	0.425

$P^s_{\pm}(r,t)$ displayed in Fig. 4. We note parenthetically that the $H^s_c(r_0)=0$ in each case yields an r_0 (Ga, 0.16; K, 0.21; hard sphere; 0.17) that describes a constant (in time) probability density $P^s_{\pm}(r,t)$; this r_0 can easily be verified to be the interception of $P^s_{\pm}(r,t)$ given in Fig. 4.

IV. CONCLUSION

To summarize, we have applied idealized MCT to liquid metal Ga to study its dynamic properties within the β-relaxation regime. We find that the occurrence of temporally fluctuating bonded-pair atomic clusters in the supercooled states of Ga has significant effects on the dynamic behavior. The most succinct feature is the appearance of a double-peaked $P^s_{\pm}(r,t)$. This latter characteristic is interpreted here as due to the presence of intimately associated bonded-pairs atoms in the 1201-, 1311-, and 1301-type clusters which play the role of inducing a different bond-hindered mechanism in addition to the caged-diffused mechanism. Two immediate consequences follow. The first consequence is that the calculated λ parameter does not follow the expected decreasing trend, but instead has a value more compatible with the trend of most experimentally observed glass-forming materials whose fitted λ's tend to be large (~ 0.8). The second consequence is the discernible influences on the time evolution of tagged particle $P^s_-(r,t)$ which shows a much slower retarded motion compared with other simple monatomic systems. In view of this sluggish behavior, the Ga system may be a good candidate for investigating the long-lived metastable liquid states currently of great interest in the literature [19,20].

ACKNOWLEDGMENTS

This work was partially supported by the National Science Council, Taiwan, Republic of China (Grant No. NSC86-2112-M008-002). We thank Professor S. F. Tsai for providing us with the data of pair correlation functions and for stimulating discussions. We are grateful to the National Center for High-Performance Computing, Taiwan, Republic of China for the support of the computing facilities.

[1] G. Li, M. Du, X. K. Chen, and H. Z. Cummins, Phys. Rev. A **45**, 3867 (1992); G. Li, M. Du, J. Hernandez, and H. Z. Cummins, Phys. Rev. E **48**, 1192 (1993); H. Z. Cummins, W. M. Du, M. Fuchs, W. Götze, S. Hilderbrand, A. Latz, G. Li, and N. J. Tao, *ibid.* **47**, 4223 (1993); J. Wuttke, M. Kiebel, E. Bartsch, F. Fujara, W. Petry, and H. Sillescu, Z. Phys. B **91**, 357 (1993).

[2] U. Bengtzelius, W. Götze, and A. Sjölander, J. Phys. C **17**, 5915 (1984).

[3] W. Götze, in *Liquids, Freezing and Glass Transition*, edited by J. P. Hansen, D. Levesque, and J. Zinn-Justin (North-Holland, Amsterdam, 1991); W. Götze and L. Sjögren, Rep. Prog. Phys. **55**, 241 (1992).

[4] W. Kob and H. C. Andersen, Phys. Rev. Lett. **73**, 1376 (1994).

[5] M. Nauroth and W. Kob (unpublished).

[6] J. N. Roux, J. L. Barrat, and J. P. Hansen, J. Phys.: Condens. Matter **1**, 7171 (1989).

[7] S. K. Lai and H. C. Chen, J. Phys.: Condens. Matter **5**, 4325 (1993).

[8] S. K. Lai and H. C. Chen, J. Phys.: Condens. Matter **7**, 1499 (1995); S. K. Lai and S. Y. Chang, Phys. Rev. B **51**, R12 869 (1995).

[9] J. L. Barrat, W. Götze, and A. Latz, J. Phys. Condens. Matter **1**, 7163 (1989).

[10] W. J. Ma and S. K. Lai, Physica B **233**, 221 (1997).

[11] W. J. Ma and S. K. Lai, Phys. Rev. E **55**, 2026 (1997).

[12] A. Bererhl, L. Bosio, and R. Cortes, J. Non-Cryst. Solids **30**, 253 (1979).

[13] S. F. Tsay, Phys. Rev. B **48**, 5945 (1993); **50**, 103 (1994).

[14] G. F. Signorini, J. L. Barrat, and M. L. Klein, J. Chem. Phys. **92**, 1294 (1990).

[15] H. R. Wendt and F. F. Abraham, Phys. Rev. Lett. **41**, 1244 (1978).

[16] J. D. Honeycutt and H. C. Andersen, J. Phys. Chem. **91**, 4950 (1987). Hereafter we follow the nomenclature of this reference and characterize the atomic bonded-pair clusters by a sequence of four integers. They are defined as follows. Let us call a pair of atoms of interest the ''root pair'' and denote them by solid circles. The so-called bonding of root pair atoms is defined by some cutoff distance, which is here taken to be the first minimum distance $r_{1,\min}$ of $g(r)$. We assign the first integer 1 when the root pair has a ''bond length'' $r \leqslant r_{1,\min}$ (depicted by a full line) and 2 otherwise (shown as a dashed line). The second integer represents the number of near neighbors (indicated by open circles) common and each bonded to the root pair. The third integer gives the number of atomic bonds (subject to the same cutoff distance) between the common neighbors. These three numbers are not sufficient to specify a diagram uniquely. A fourth integer is therefore introduced so that one can provide a unique correspondence between the arrangement of atomic bonds and diagrams.

[17] M. Fuchs, W. Götze, S. Hildebrand, and A. Latz, Z. Phys. B **87**, 43 (1992).

[18] For a tagged particle in any of the three types of temporally fluctuating atomic bonded pairs, the surrounding atoms (about nine in number) are located on the average at the first nearest neighbor $r_{1,\max}=1.03\sigma$ of $g(r)$ but can straddle a bit to the first minimum position $r_{1,\min}=1.24\sigma$ for a distance $1.24\sigma - 1.03\sigma \simeq 0.21\sigma$, since the cutoff bond length (see Ref. [16]) is here taken to satisfy $r \leqslant r_{1,\min}$. This region is roughly the separation of the first and second peaks of $P^s_{\pm}(r,t)$. In the 1551-type atomic clusters there are five bonded common neighbors to the root pair and thus are geometrically constrained to straddle making the occurrence of the $P^s_{\pm}(r^{(2)}_{\max},t)$ much less likely. Note that the coordination number for this latter type for K is approximately 13, which further reduces straddling.

[19] W. J. Ma and S. K. Lai (unpublished).

[20] A. Ha, I. Cohen, X. Zhao, M. Lee, and D. Kivelson, J. Phys. Chem. **100**, 1 (1996); **100**, 8518 (1996).